Non-relativistic bound states in a moving thermal bath

Miguel A. Escobedo

Physik-Department T30f. Technische Universität München

15th of June, 2011

arXiv [1105.1249]. Work done in collaboration with Massimo Mannarrelli and Joan Soto.

Outline

- Introduction

EFT for bound states at finite temperature

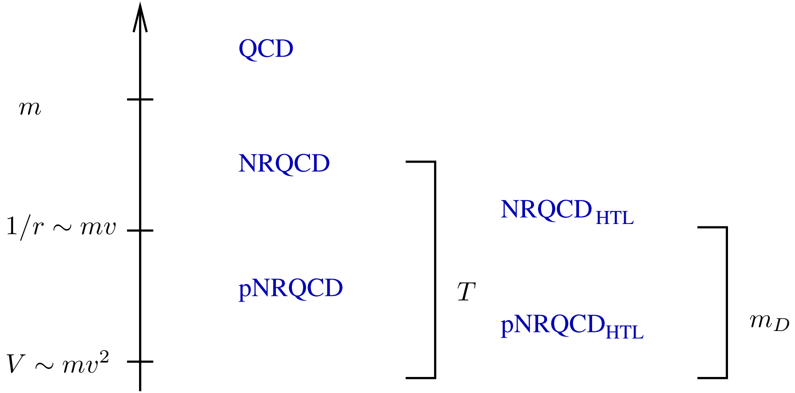

Imaginary part of the potential

For $T \gg \frac{1}{r} \sim gT$

$$V(r) = -\frac{4\alpha_{\rm s} e^{-m_D r}}{3r} - i\frac{4\alpha_{\rm s} C_F T \phi(m_D r)}{3},$$

- This imaginary part of the potential was found by Laine, Philipsen, Romatschke and Tassler.
- It was confirmed by EFT techniques [Escobedo and Soto—Brambilla, Ghiglieri, Petreczky and Vairo].
- It was found that in the $g \to 0$ limit this provides the dominant dissociation mechanism.
- This temperature is smaller than the one obtained just with screening.

Ideal conditions

- The EFTs for HQ at finite temperature and the imaginary part of the potential were obtained assuming thermal equilibrium and that the bound state is at rest.
- This is not what happens in heavy-ion collisions.

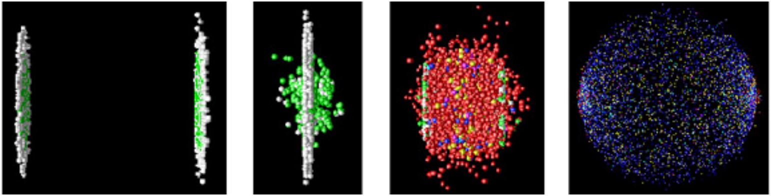

Relax this conditions

- Anisotropic plasma
- Quarkonium is moving
- ...

Relax this conditions

- Anisotropic plasma
  Burnier, Laine and Vepsälänen. Dumitru, Guo and Strickland. Philipsen and Tassler.
- Quarkonium is moving
- ...

Is quarkonium moving?

Experimentally, if quarkonium is comoving with the thermal bath then the v_2 parameter should be the same as other types of particles.

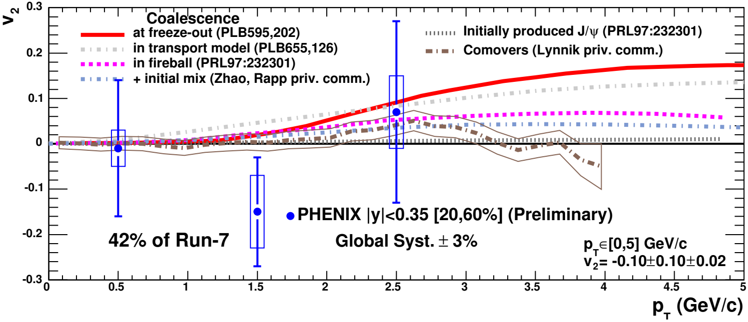

Picture taken from C. Silvestre for PHENIX collaboration, J. Phys. G35:104136 (2008)

Is quarkonium moving?

- Regeneration
- Initially produced
  - Slow down due to the plasma.
  - Dissociated while still moving with a certain velocity.

It is needed to know how dissociation behaves when there is a velocity between the bound state and the thermal bath.

General framework

We choose the frame where the bound state is at rest and the thermal bath is moving.

$$f(\beta^\mu k_\mu) = \frac{1}{e^{|\beta^\mu k_\mu|} \pm 1},$$

$$\beta^\mu = \frac{\gamma}{T}(1, \mathbf{v}) = \frac{u^\mu}{T},$$

We use a generalization of the real-time formalism called Non-equilibrium field theory (Zhou, Su, Han and Liu). At tree level substitute the equilibrium distribution functions by the non-equilibrium ones in the propagator.

Some of the identities found in equilibrium are not longer valid. For example,

$$\Delta_S = [1 + 2n_B(|k_0|)]sgn(k_0)[\Delta_R - \Delta_A]$$

Massless particles

We can define an *effective temperature* depending on the incidence angle.

$$T_{\mathrm{eff}}(\theta, v) = \frac{T\sqrt{1-v^2}}{1 - v\cos\theta}\,.$$

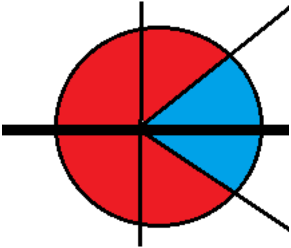

- Heavy quarkonium potential in a moving thermal bath

Heavy quarkonium potential in a thermal bath at rest

For $T \gg \frac{1}{r} \sim gT$

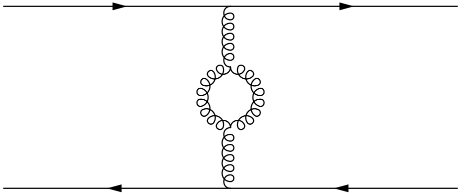

Heavy quarkonium potential in a thermal bath at rest

For $T \gg \frac{1}{r} \sim gT$

$$V(r) = -\frac{4\alpha_{\rm s} e^{-m_D r}}{3r} - i\frac{4\alpha_{\rm s} C_F T \phi(m_D r)}{3},$$

In the real-time formalism this is the Fourier transform of the time-ordered (11) propagator of longitudinal static gluons (in the Coulomb gauge). It has a real and an imaginary part.

$$\Delta_{11} = \frac{1}{2}\left(\Delta_R + \Delta_A + \Delta_S\right)$$

In equilibrium there exist a simple relation between Δ_R and Δ_S due to fluctuation-dissipation theorem. In our case this relation does not hold.

Computation of $\Pi_S^{\mu\nu}(k)$

We know

- That HTL are gauge invariant.
- That $k_\mu \Pi_S^{\mu\nu} = 0$.
- The tensor structure of $\Pi_S(k)_{\mu\nu}$ can only depend on the external momentum k^μ and the velocity of the thermal bath v^μ.

Computation of $\Pi_S^{\mu\nu}(k)$

$$\Pi_S^{\mu\nu} = \Pi_1 \left(g^{\mu\nu} - \frac{k^\mu k^\nu}{k^2} \right) + \Pi_2 \left(v^\mu - \frac{(v \cdot k) k^\mu}{k^2} \right) \left(v^\nu - \frac{(v \cdot k) k^\nu}{k^2} \right)$$

- Π_1 and Π_2 are scalars that can be computed in the thermal bath rest frame.
- Knowing this scalars it is straightforward to compute Π_S in any frame.
- For Π_R the procedure is the same.

Π_S and Π_R

$$\Pi_S(k,u) = \frac{i2\pi m_D^2 T (1-v^2)^{3/2}(1+\frac{v^2}{2}\cos^2\theta)}{|\mathbf{k}|(1-v^2\sin^2\theta)^{5/2}}$$

$$\Pi_R(k,u) = a(z) + \frac{b(z)}{1-v^2}$$

where $z = \frac{v\cos\theta}{\sqrt{1-v^2\sin^2\theta}}$

$$a(z) = \frac{m_D^2}{2}\left(z^2 - (z^2-1)\frac{z}{2}\ln\left(\frac{z+1+i\epsilon}{z-1+i\epsilon}\right)\right)$$

$$b(z) = (z^2-1)\left(a(z) - m_D^2(1-z^2)\left(1-\frac{z}{2}\ln\left(\frac{z+1+i\epsilon}{z-1+i\epsilon}\right)\right)\right)$$

Δ_R and Δ_S

In the Coulomb gauge, the propagator of the longitudinal gluon field A_0

$$\Delta_R = \frac{1}{k^2 + \Pi_R(k)}$$

$$\Delta_A = (\Delta_R)^*$$

$$\Delta_S = \frac{\Pi_S}{2iIm\Pi_R}(\Delta_R - \Delta_A)$$

It can be shown that the following relation is only fulfilled for $v = 0$.

$$\Delta_S = (1 + 2n_B(|k_0|))sgn(k_0)(\Delta_R - \Delta_A)$$

- The real part of the potential

The real part of the potential

$$V(r) = \frac{1}{2}(V_R(r) + V_A(r))$$

- This was computed before by Chu and Matsui.
- It can serve us to check the accuracy of our numerical computations.
- Nowadays the velocity reached experimentally is expected to be much higher.
- It is interesting to compare to AdS/CFT correspondence results.

AdS/CFT correspondence results

It was found by H. Liu, K. Rajagopal and U.A. Wiedemann that the potential in Super Yang-Mills was Yukawa like with

$$m_D(v,\theta) = m_D(0,0)\frac{h(v,\theta)}{(1-v^2)^{1/4}},$$

with $h(v,\theta) \sim 1$.

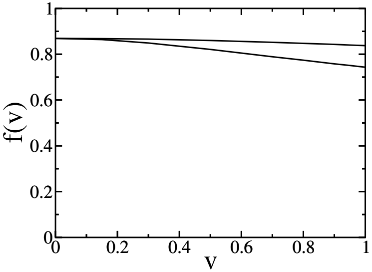

AdS/CFT correspondence results

It was found by H. Liu, K. Rajagopal and U.A. Wiedemann that the potential in Super Yang-Mills was Yukawa like with

$$m_D(v,\theta) = m_D(0,0)\frac{h(v,\theta)}{(1-v^2)^{1/4}},$$

with $h(v,\theta) \sim 1$.

- Screening enhances with the velocity.
- The potential is still very isotropic.

The real part of the potential, normalization

At $v = 0$

$$Re\, V(r) = -\frac{4\alpha_{\rm s} e^{-m_D r}}{3r} = -\frac{4\alpha_{\rm s} C_F m_D g(m_D r)}{3}$$

at any velocity we can define

$$g(m_D r) = -\frac{3 Re V(r)}{4\alpha_{\rm s} m_D}$$

$g(x)$ does not depend on T, it is useful to compare the same T with different v. This is what we are going to plot.

The real part of the potential at $v = 0$

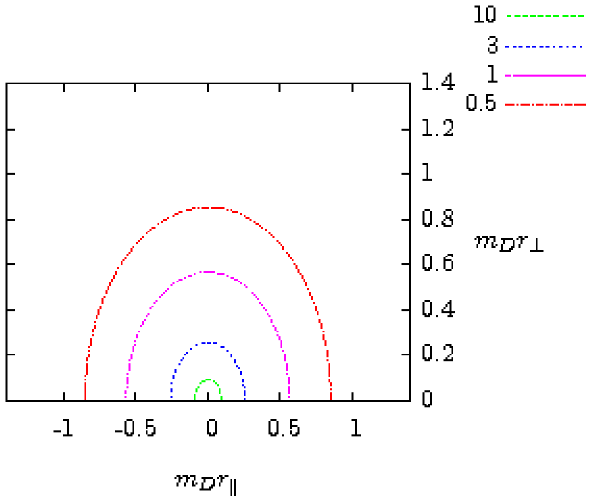

The real part of the potential at $v = 0.5$

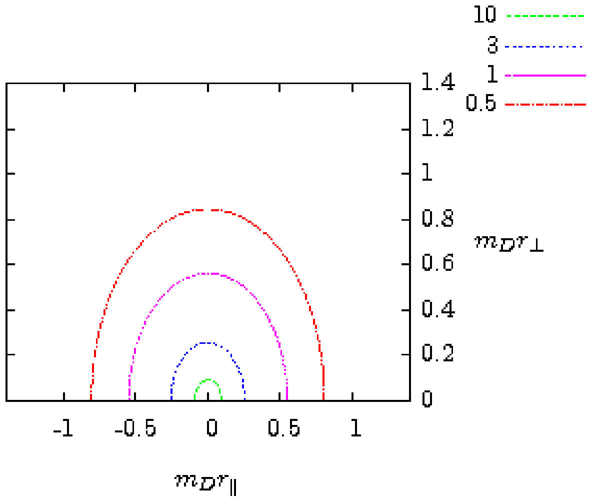

The real part of the potential at $v = 0.9$

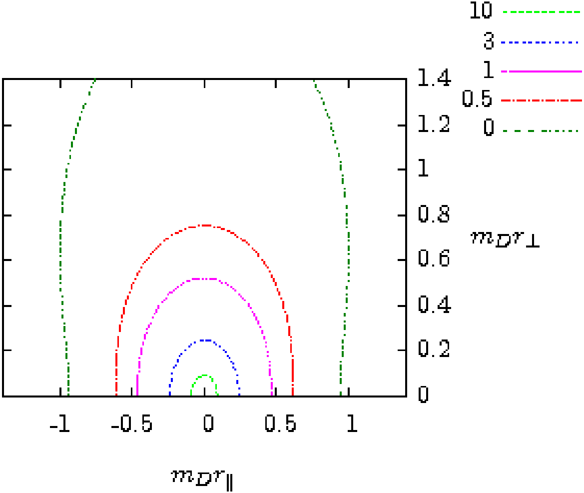

The real part of the potential at $v = 0.99$

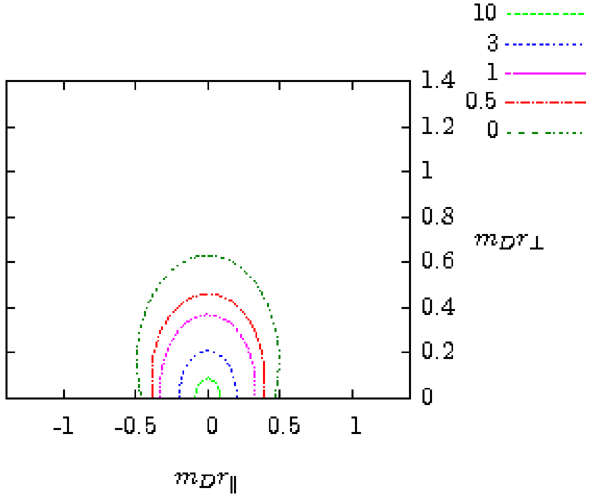

Analysis of the plots

- The closer the lines the stronger the screening.
- A Yukawa potential does not provide a good fit, specially in the direction parallel to the velocity of the thermal bath.
- Screening and anisotropy grow with the velocity.
- The weak coupling behavior is very different to the proposed by AdS/CFT.

The wake

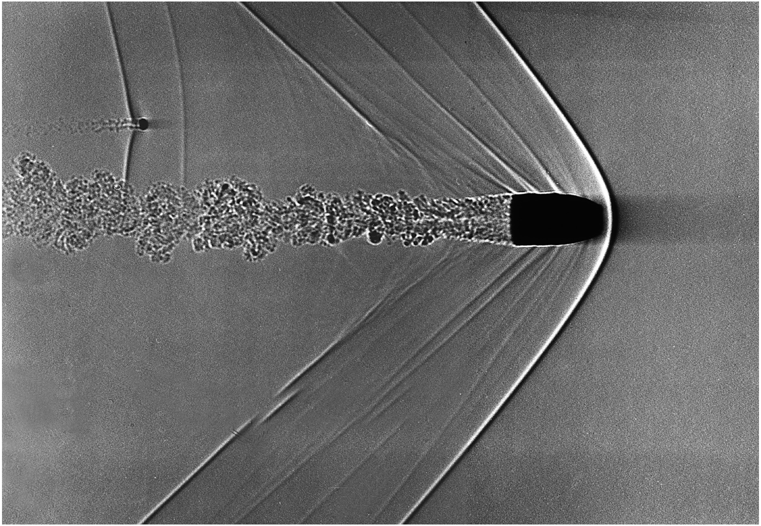

The wake

- A wake is a density fluctuation produced by the fact that an object is moving at a high speed in a medium.
- The fact that bound states moving in a medium produce a wake is known in condensed matter physics (P. M. Echenique, F. Flores and R. H. Ritchie).
- It has also been predicted in the quark-gluon plasma. Both in weak coupling approximation and AdS/CFT correspondence (N. Armesto. M. G. Mustafa, M. H. Thoma, P. Chakraborty. J. Ruppert and B. Muller, B. F. Jiang and J. R. Li, P. M. Chesler and L. G. Yaffe).
- Our approach is slightly different because we work in the frame where the bound state is at rest.

Wake in the parallel direction

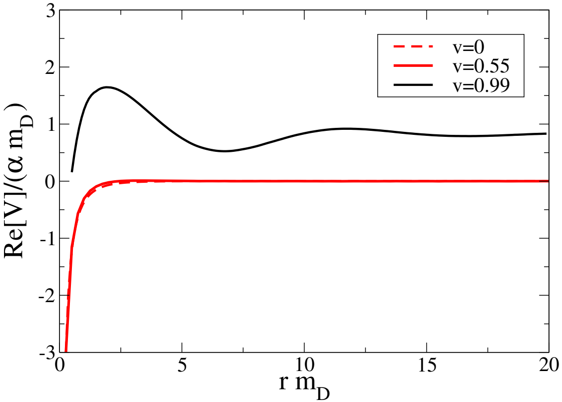

No wake in the perpendicular direction

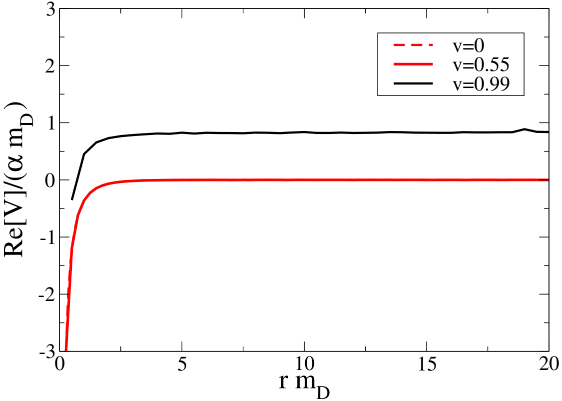

- The imaginary part of the potential

The imaginary part of the potential at $v = 0$

$$Im\,V(r) = V_S(r) = -\frac{4\alpha_s T \phi(m_D r)}{3},$$

with

$$\phi(x) = 2\int_0^\infty \frac{dzz}{(z^2+1)^2}\left(1 - \frac{\sin(zx)}{zx}\right).$$

At any velocity we can define

$$\phi(m_D r) = -\frac{3 Im\,V(r)}{4\alpha_s T}.$$

This is what we are going to plot.

The imaginary part of the potential at $v = 0$

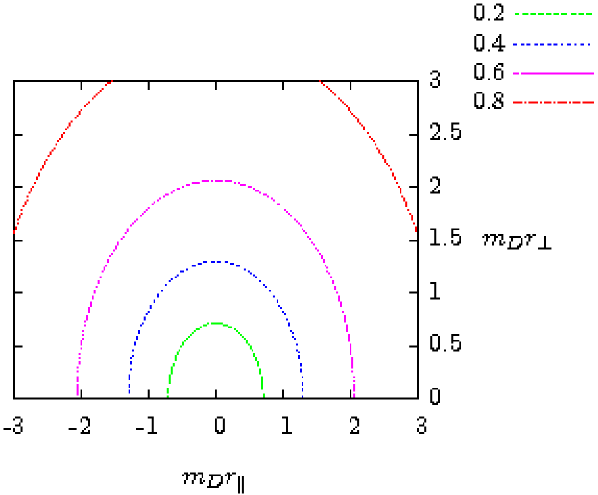

The imaginary part of the potential at $v = 0.5$

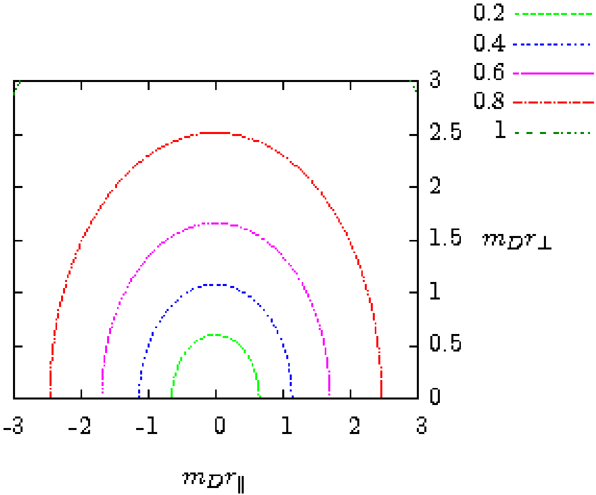

The imaginary part of the potential at $v = 0.9$

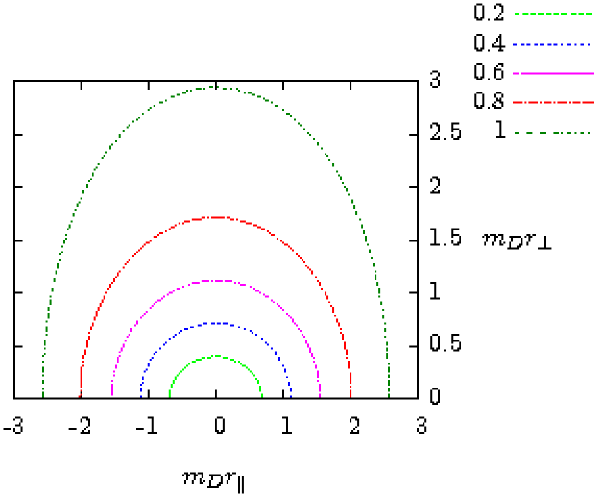

The imaginary part of the potential at $v = 0.99$

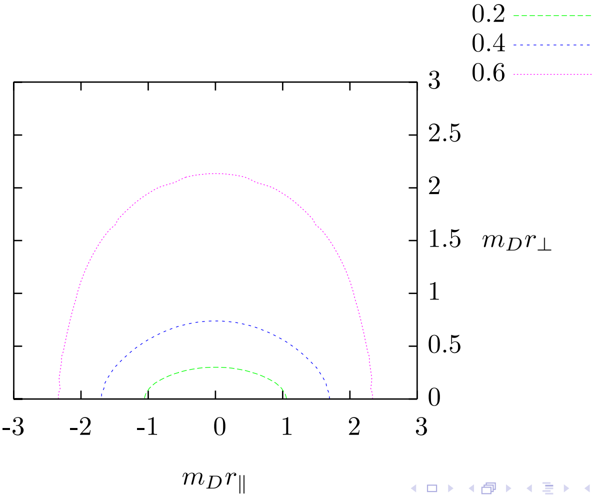

The imaginary part in the parallel direction

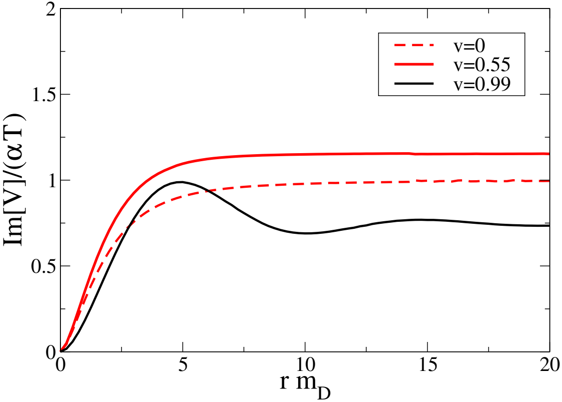

The imaginary part in the perpendicular direction

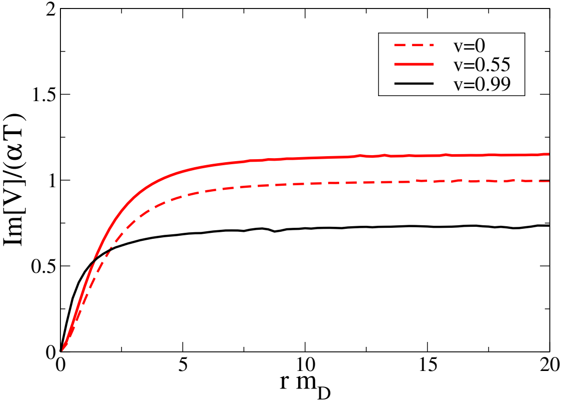

Analysis of the results

- The imaginary part grows with the velocity up to $v \sim 0.9$ but after it starts decreasing.
- There is a large anisotropy.
- For most velocities it would still be the dominant dissociation mechanism. But for relativistic velocities?.

Intuitive explanation for anisotropy

- The heavy quark and the heavy anti-quark interchange gluons with $k_0 \ll k \sim \frac{1}{r}$.
- The travel of this gluon from the heavy quark to the heavy anti-quark can be interrupted by the collision with particles in the thermal bath. This particles are on-shell and have typical energy πT.
- By momentum conservation this can only happen for particles of the thermal bath that come from the perpendicular direction.

Intuitive explanation for anisotropy

In the parallel direction

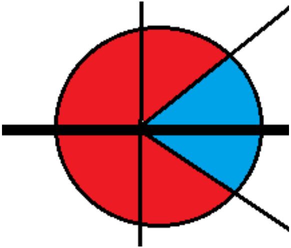

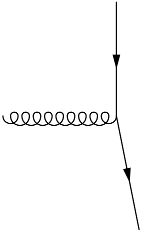

Most of the scattering come from red-shifted particles.

Intuitive explanation for anisotropy

In the perpendicular direction

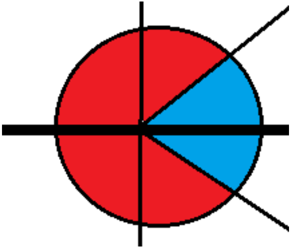

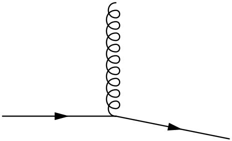

There is also an important contribution from blue-shifted particles.

- The relativistic case.

The energy scales

There are

- The typical momentum p.
- The Debye mass scale m_D.
- A scale related with the imaginary part of the potential m_d.

Then

- If $p \gg m_D, m_d$ the bound state survives.
- If $p \sim m_d \gg m_D$ it dissociates due to the imaginary part.
- If $p \sim m_D \gg m_d$ it dissociates due to screening.

The energy scales

	m_D	m_d
$v = 0$	gT	$g^{2/3}T$
$v \to 1$ and $\theta \nsim \frac{\pi}{2}$	gT	$g^{2/3}T\sqrt{1-v^2}$
$v \to 1$ and $\theta \sim \frac{\pi}{2}$	$\frac{gT}{\sqrt{1-v^2}}$	$\frac{g^{2/3}T}{(1-v^2)^{1/3}}$

For very high velocities screening substitutes the imaginary part as the dissociation mechanism in the weak coupling.
For generic angles, the critical velocity where this change of behavior is observed is

$$v_c \sim \sqrt{1 - ag^{2/3}}$$

- Non-relativistic EFT in a moving thermal bath.

Non-relativistic EFT in a thermal bath

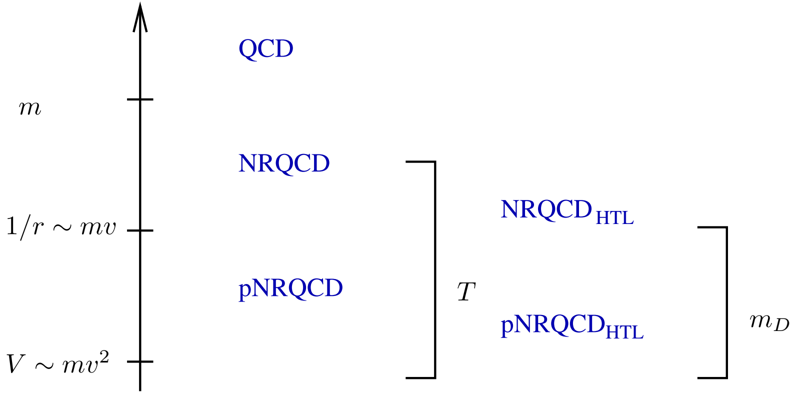

The distribution function

We choose the frame where the bound state is at rest and the thermal bath is moving.

$$f(\beta^\mu k_\mu) = \frac{1}{e^{|\beta^\mu k_\mu|} \pm 1},$$

$$\beta^\mu = \frac{\gamma}{T}(1, \mathbf{v}) = \frac{u^\mu}{T},$$

Massless particles

We can define an *effective temperature* depending on the incidence angle.

$$T_{\rm eff}(\theta, v) = \frac{T\sqrt{1-v^2}}{1-v\cos\theta}\,.$$

If $v \sim 1$ the order of magnitude of $T_{\rm eff}$ can depend of θ.

Light-cone coordinates

$$k_+ = k_0 + k_3 \qquad \text{and} \qquad k_- = k_0 - k_3 \,.$$

$$\beta^\mu k_\mu = \frac{1}{2}\left(\frac{k_+}{T_+} + \frac{k_-}{T_-}\right) ,$$

$$T_+ = T\sqrt{\frac{1+v}{1-v}} \qquad \text{and} \qquad T_- = T\sqrt{\frac{1-v}{1+v}} \,.$$

Remarks

- These equations are true for any dispersion relation.
- For a massive particle with mass M, the minimum of $\beta^\mu k_\mu$ is $\frac{M}{T}$. If $M \gg T$ this particle is not found in the thermal bath.
- If $v \sim 1$ then $T_+ \gg T_-$. This is an interesting case for an EFT analysis. It is also useful because it will allow to resum large logarithms.

Degrees of freedom

$$\beta^\mu k_\mu = \frac{1}{2}\left(\frac{k_+}{T_+} + \frac{k_-}{T_-}\right) ,$$

- If $k_+ \gg T_+$ or $k_- \gg T_-$ thermal effects are exponentially suppressed.
- A collinear region, corresponding to $k_+ \sim T_+$ and $k_- \lesssim T_-$, the bulk of particles in the thermal bath.
- An ultrasoft region, corresponding to $k_+ \ll T_+$ and $k_- \lesssim T_-$, particles of the thermal bath whose energy is similar to that of the bound state.

Taking into account this collinear region terms similar to the ones found in Soft Collinear Effective Theory appear.

Hydrogen atom for $m_e \sim T_+ \gg m\alpha \gg T_- \gg m\alpha^2$

- $T = \sqrt{T_+ T_-}$ then $m_e \gg T$. There are only photons in the thermal bath.
- The matching between QED and NRQED has to be done taking into account the existence of collinear photons.
- The collinear photons have to be integrated out in the matching between NRQED and pNRQED because their virtuality is of order T^2.
- Ultrasoft photons effects can be computed in pNRQED.

Collinear photons in the matching between QED and NRQED

$\frac{1}{2}\frac{1+\gamma_0}{2}\Bigg($ 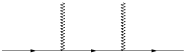 $+$ 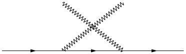 $\Bigg)\frac{1+\gamma_0}{2} =$

$\sqrt{Z}\frac{1+\gamma_0}{2}$ 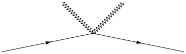 $\sqrt{Z}$

Because in NRQED the following diagram is not possible

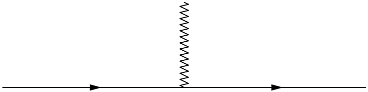

by momentum conservation in each vertex a non-relativistic electron can not receive a collinear photon and keep being non-relativistic.

The collinear sector of the NRQED Lagrangian

$$
\begin{aligned}
\delta\mathcal{L}_{NRQED} = {} & c_1\frac{\psi^\dagger\psi}{m_e}\frac{\bar{n}^\mu F_{\mu i}}{(\bar{n}\partial)}\frac{\bar{n}^\nu F_{\nu i}}{(\bar{n}\partial)} + c_2\frac{\psi^\dagger\psi}{m_e}\frac{\bar{n}^\mu n^\nu F_{\mu\nu}}{(\bar{n}\partial)}\frac{\bar{n}^\alpha n^\beta F_{\alpha\beta}}{(\bar{n}\partial)} \\
& + c_3\frac{\psi^\dagger\psi}{m_e}\left[\frac{n^\mu F_{i\mu}}{(\bar{n}\partial)}\frac{\bar{n}^\nu F_{\nu i}}{(\bar{n}\partial)} + \frac{\bar{n}^\mu F_{i\mu}}{(\bar{n}\partial)}\frac{n^\nu F_{\nu i}}{(\bar{n}\partial)}\right] \\
& + \frac{ic_4}{m_e^2}\left[\psi^\dagger\frac{\bar{n}^\mu n^\nu F_{\mu\nu}}{(\bar{n}\partial)}\frac{\bar{n}^\alpha n^\beta F_{\alpha\beta}}{(\bar{n}\partial)}D_3\psi - D_3\psi^\dagger\frac{\bar{n}^\mu n^\nu F_{\mu\nu}}{(\bar{n}\partial)}\frac{\bar{n}^\alpha n^\beta F_{\alpha\beta}}{(\bar{n}\partial)}\psi\right] \\
& + \frac{ic_5}{m_e^2}\left(\psi^\dagger\left[\frac{\bar{n}^\mu n^\nu F_{\mu\nu}}{(\bar{n}\partial)}\frac{\bar{n}^\alpha F_{\alpha i}}{(\bar{n}\partial)} + \frac{\bar{n}^\mu F_{\mu i}}{(\bar{n}\partial)}\frac{\bar{n}^\alpha n^\beta F_{\alpha\beta}}{(\bar{n}\partial)}\right]D_i\psi\right. \\
& \left. D_i\psi^\dagger\left[\frac{\bar{n}^\mu n^\nu F_{\mu\nu}}{(\bar{n}\partial)}\frac{\bar{n}^\alpha F_{\alpha i}}{(\bar{n}\partial)} + \frac{\bar{n}^\mu F_{\mu i}}{(\bar{n}\partial)}\frac{\bar{n}^\alpha n^\beta F_{\alpha\beta}}{(\bar{n}\partial)}\right]\psi\right) + c_6\frac{\psi^\dagger\psi}{m_e}\frac{n^\mu F_{i\mu}}{(\bar{n}\partial)}\frac{n^\nu F_{i\nu}}{(\bar{n}\partial)} \\
& + c_7\frac{\psi^\dagger\psi}{m_e}\left[\frac{\bar{n}^\mu\partial_- F_{\mu i}}{(\bar{n}\partial)^2}\frac{\bar{n}^\nu F_{\nu i}}{(\bar{n}\partial)} + \frac{\bar{n}^\mu F_{\mu i}}{(\bar{n}\partial)}\frac{\bar{n}^\nu\partial_- F_{\nu i}}{(\bar{n}\partial)^2}\right] \\
& + c_8\frac{\psi^\dagger\psi}{m_e}\left[\frac{\bar{n}^\mu n^\nu\partial_- F_{\mu\nu}}{(\bar{n}\partial)^2}\frac{\bar{n}^\alpha n^\beta F_{\alpha\beta}}{(\bar{n}\partial)} + \frac{\bar{n}^\mu n^\nu F_{\mu\nu}}{(\bar{n}\partial)}\frac{\bar{n}^\alpha n^\beta\partial_- F_{\alpha\beta}}{(\bar{n}\partial)^2}\right] \\
& + \frac{ic_9}{m_e^2}\left(D_i\psi^\dagger\left[\frac{\bar{n}^\mu F_{\mu j}}{(\bar{n}\partial)}\frac{\bar{n}^\nu\partial_j F_{\nu i}}{(\bar{n}\partial)^2} + \frac{\bar{n}^\mu\partial_j F_{\mu j}}{(\bar{n}\partial)^2}\frac{\bar{n}^\nu F_{\nu j}}{(\bar{n}\partial)}\right]\psi\right. \\
& \left. -\psi^\dagger\left[\frac{\bar{n}^\mu F_{\mu j}}{(\bar{n}\partial)}\frac{\bar{n}^\nu\partial_j F_{\nu i}}{(\bar{n}\partial)^2} + \frac{\bar{n}^\mu\partial_j F_{\mu j}}{(\bar{n}\partial)^2}\frac{\bar{n}^\nu F_{\nu j}}{(\bar{n}\partial)}\right]D_i\psi\right) \\
& + \frac{ic_{10}}{m_e^2}\left(D_i\bar{\psi}\left[\frac{n^\mu F_{i\mu}}{(\bar{n}\partial)}\frac{\bar{n}^\nu n^\alpha F_{\nu\alpha}}{(\bar{n}\partial)} + \frac{\bar{n}^\mu n^\nu F_{\mu\nu}}{(\bar{n}\partial)}\frac{n^\alpha F_{i\alpha}}{(\bar{n}\partial)}\right]\psi\right. \\
& \left. -\psi^\dagger\left[\frac{n^\mu F_{i\mu}}{(\bar{n}\partial)}\frac{\bar{n}^\nu n^\alpha F_{\nu\alpha}}{(\bar{n}\partial)} + \frac{\bar{n}^\mu n^\nu F_{\mu\nu}}{(\bar{n}\partial)}\frac{n^\alpha F_{i\alpha}}{(\bar{n}\partial)}\right]D_i\psi\right) \\
& + \frac{1}{m_e^3}\left(D_{jj}^2\psi^\dagger\left[c_{11}\frac{\bar{n}^\mu F_{\mu i}}{(\bar{n}\partial)}\frac{\bar{n}^\nu F_{\nu i}}{(\bar{n}\partial)} + c_{12}\frac{\bar{n}^\mu n^\nu F_{\mu\nu}}{(\bar{n}\partial)}\frac{\bar{n}^\alpha n^\beta F_{\alpha\beta}}{(\bar{n}\partial)}\right]\psi\right. \\
& \left. +\psi^\dagger\left[c_{11}\frac{\bar{n}^\mu F_{\mu i}}{(\bar{n}\partial)}\frac{\bar{n}^\nu F_{\nu i}}{(\bar{n}\partial)} + c_{12}\frac{\bar{n}^\mu n^\nu F_{\mu\nu}}{(\bar{n}\partial)}\frac{\bar{n}^\alpha n^\beta F_{\alpha\beta}}{(\bar{n}\partial)}\right]D_{jj}^2\psi\right) \\
& + \frac{1}{m_e^3}D_j\psi^\dagger\left[c_{13}\frac{\bar{n}^\mu F_{\mu i}}{(\bar{n}\partial)}\frac{\bar{n}^\nu F_{\nu i}}{(\bar{n}\partial)} + c_{14}\frac{\bar{n}^\mu n^\nu F_{\mu\nu}}{(\bar{n}\partial)}\frac{\bar{n}^\alpha n^\beta F_{\alpha\beta}}{(\bar{n}\partial)}\right]D_j\psi \\
& + \frac{c_{15}}{m_e^3}\left(D_{33}^2\psi^\dagger\frac{\bar{n}^\mu n^\nu F_{\mu\nu}}{(\bar{n}\partial)}\frac{\bar{n}^\alpha n^\beta F_{\alpha\beta}}{(\bar{n}\partial)}\psi + \psi^\dagger\frac{\bar{n}^\mu n^\nu F_{\mu\nu}}{(\bar{n}\partial)}\frac{\bar{n}^\alpha n^\beta F_{\alpha\beta}}{(\bar{n}\partial)}D_{33}^2\psi\right) \\
& + \frac{c_{16}}{m_e^3}D_3\psi^\dagger\frac{\bar{n}^\mu n^\nu F_{\mu\nu}}{(\bar{n}\partial)}\frac{\bar{n}^\alpha n^\beta F_{\alpha\beta}}{(\bar{n}\partial)}D_3\psi \\
& + \frac{c_{17}}{m_e^3}\left(D_{3i}^2\psi^\dagger\left[\frac{\bar{n}^\mu n^\nu F_{\mu\nu}}{(\bar{n}\partial)}\frac{\bar{n}^\alpha F_{\alpha i}}{(\bar{n}\partial)} + \frac{\bar{n}^\mu F_{\mu i}}{(\bar{n}\partial)}\frac{\bar{n}^\nu n^\alpha F_{\nu\alpha}}{(\bar{n}\partial)}\right]\psi\right. \\
& -D_3\psi^\dagger\left[\frac{\bar{n}^\mu n^\nu F_{\mu\nu}}{(\bar{n}\partial)}\frac{\bar{n}^\alpha F_{\alpha i}}{(\bar{n}\partial)} + \frac{\bar{n}^\mu F_{\mu i}}{(\bar{n}\partial)}\frac{\bar{n}^\nu n^\alpha F_{\nu\alpha}}{(\bar{n}\partial)}\right]D_i\psi \\
& -D_i\psi^\dagger\left[\frac{\bar{n}^\mu n^\nu F_{\mu\nu}}{(\bar{n}\partial)}\frac{\bar{n}^\alpha F_{\alpha i}}{(\bar{n}\partial)} + \frac{\bar{n}^\mu F_{\mu i}}{(\bar{n}\partial)}\frac{\bar{n}^\nu n^\alpha F_{\nu\alpha}}{(\bar{n}\partial)}\right]D_3\psi \\
& \left. +\psi^\dagger\left[\frac{\bar{n}^\mu n^\nu F_{\mu\nu}}{(\bar{n}\partial)}\frac{\bar{n}^\alpha F_{\alpha i}}{(\bar{n}\partial)} + \frac{\bar{n}^\mu F_{\mu i}}{(\bar{n}\partial)}\frac{\bar{n}^\nu n^\alpha F_{\nu\alpha}}{(\bar{n}\partial)}\right]D_{3i}^2\psi\right).
\end{aligned}
$$

The collinear sector of the NRQED Lagrangian. Coulomb gauge

- Collinear A_0 propagator is not affected by the temperature.
- $\nabla \mathbf{A} = 0$. For collinear photons this also implies $A_3 \ll |\mathbf{A}_\perp|$.

The collinear sector of the NRQED Lagrangian. Coulomb gauge.

$$\delta\mathcal{L}_{NRQED} = c_1\frac{\psi^\dagger\psi}{m_e}\frac{\bar{n}^\mu F_{\mu i}}{(\bar{n}\partial)}\frac{\bar{n}^\nu F_{\nu i}}{(\bar{n}\partial)} + c_2\frac{\psi^\dagger\psi}{m_e}\frac{\bar{n}^\mu n^\nu F_{\mu\nu}}{(\bar{n}\partial)}\frac{\bar{n}^\alpha n^\beta F_{\alpha\beta}}{(\bar{n}\partial)}$$

[redacted]

$$+\frac{1}{m_e^3}\Big(D_{jj}^2\psi^\dagger\Big[c_{11}\frac{\bar{n}^\mu F_{\mu i}}{(\bar{n}\partial)}\frac{\bar{n}^\nu F_{\nu i}}{(\bar{n}\partial)} + \text{[redacted]}\Big]\psi$$

$$+\psi^\dagger\Big[c_{11}\frac{\bar{n}^\mu F_{\mu i}}{(\bar{n}\partial)}\frac{\bar{n}^\nu F_{\nu i}}{(\bar{n}\partial)} + \text{[redacted]}\Big]D_{jj}^2\psi\Big)$$

$$+\frac{1}{m_e^3}D_j\psi^\dagger\Big[c_{13}\frac{\bar{n}^\mu F_{\mu i}}{(\bar{n}\partial)}\frac{\bar{n}^\nu F_{\nu i}}{(\bar{n}\partial)} + \text{[redacted]}\Big]D_j\psi$$

[redacted]

Effect of collinear photons in pNRQED

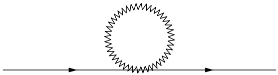

$$= -\frac{i\pi\alpha T^2}{3m_e}\left(1 - \frac{p^2}{2m_e^2}\right)$$

$$m_e^{pNRQED} = m_e + \frac{\pi\alpha T^2}{3m_e}$$

Ultrasoft photons

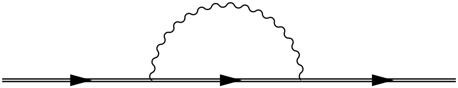

But now there is a space anisotropy

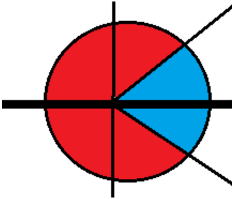

This means that the results are different depending on the third component of the angular momentum.

Ultrasoft photons.

S-wave

$$\delta E^{us}_{n00} = \delta E^{us}_{n00}|_{v=0} - \frac{4Z\alpha^2}{3}\left(1+\frac{1}{2}\log\left(\frac{1-v}{1+v}\right)\right)\frac{|\phi_n(0)|^2}{m_e^2}$$

$$\delta\Gamma^{us}_{n00} = \frac{4Z^2\alpha^3 T}{3n^2}\sqrt{\frac{1-v}{1+v}}\log\left(\frac{1+v}{1-v}\right).$$

Non s-wave

$$\delta E^{us}_{nlm} = \delta E^{us}_{nlm}|_{v=0} - \frac{Z^3\alpha^2\langle 2l00|l0\rangle\langle 2l0m|lm\rangle}{6\pi m_e^2 a_0^3 l(l+\frac{1}{2})(l+1)},$$

$$\delta\Gamma^{us}_{nlm} = \frac{4Z^2\alpha^3 T}{3n^2}\sqrt{\frac{1-v}{1+v}}\left(\log\left(\frac{1+v}{1-v}\right)\right.$$
$$\left. - \left(\log\left(\frac{1+v}{1-v}\right)-3\right)\langle 2l00|l0\rangle\langle 2l0m|lm\rangle\right).$$

Discussion

- I have chosen to present only a very specific set of temperatures and velocities.
- We have computed the case of hydrogen atom for $m_e \gg T$ at an arbitrary velocity.
- For this we achieve the same accuracy as at $v = 0$.
- This work paves the way for future developments in HQ, where complications due to vacuum polarization have to be taken into account.

- Conclusions.

Conclusions

- The EFT analysis of bound-states can be generalized to a moving thermal bath at it allows to reveal the physics in an easier and more systematic way.
- The screening becomes more important as the temperature increases, being more important than the imaginary part for $v \gg v_c$.
- The imaginary part will be the dominant dissociation mechanism for moderate velocities.
- In the case of hydrogen atom a accuracy of the order of the Lamb shift can be reached with this methods.